Plasma Current Generation and Sustainment by Electron Cyclotron Waves in the WT-2 Tokamak

A. Ando, K. Ogura, H. Tanaka, M. Iida, S. Ide, K. Oho, S. Ozaki, M. Nakamura,[a] T. Cho,[b] T. Maekawa, Y. Terumichi, and S. Tanaka

Department of Physics, Faculty of Science, Kyoto University, Kyoto 606, Japan

(Received 15 January 1986)

By injection of microwave power P_{EC} near the electron cyclotron (EC) frequency into an Ohmically heated (OH) plasma in the WT-2 tokamak after OH power is shut off, the plasma current is sustained and ramped up by the EC wave only, without OH power. Here, EC-driven current is generated by EC heating of the suprathermal electron beam in OH plasma. Further, when P_{EC} is injected into plasma sustained by lower-hybrid- (LH-) driven current, the plasma current and its rampup rate increase. Here, EC-driven current is generated by EC heating of the mildly relativistic electrons in LH-driven plasma.

PACS numbers: 52.50.Gj, 52.55.Fa

Recently, noninductive current drive (CD) has received much attention in relation to realization of the steady-state operation of tokamak reactors.[1] Experiments have shown that the plasma current is started up, ramped up, and sustained by the lower-hybrid (LH) wave in many tokamaks.[2-9] Meanwhile, other noninductive CD methods have been suggested theoretically.[1] Fisch and co-workers[10,11] have predicted that the plasma current can be produced by the quasilinear cyclotron damping of the electron cyclotron (EC) wave. This current drive, ECCD, is achieved by the creation of an asymmetric electron distribution function along the field, whose mechanism is quite different from LHCD.[1] There have been no publications of ECCD experiments apart from the observation of weak EC-driven current in the Ohmically heated (OH) discharge in the Tosca tokamak.[12] In this Letter we report the first experiment in the WT-2 tokamak, in which the plasma is sustained by the EC-driven current only, without the OH power. Further, plasma current is produced by EC heating of the mildly relativistic electron beam present in LH-current-sustained plasma.

The WT-2 tokamak[2,6] has an aluminum shell and an iron core, with major and minor radii $R_0 = 40$ and $a = 9$ cm, respectively. Microwaves from a gyrotron ($\omega/2\pi = 35.6$ GHz, $P_{EC} \leq 120$ kW, pulse width $t \leq 10$ ms) are fed from the low-field side through circular waveguides to a Vlasov antenna with parabolic reflector placed along the major radius. By rotation of the antenna around the guide axis, a linearly polarized electromagnetic wave, propagating parallel or antiparallel to the toroidal field B_T with an angle of $\pm 48°$ to B_T, is radiated as the extraordinary (X) mode. Further, an electromagnetic wave propagating perpendicular to B_T is injected as the ordinary (O) mode. Also microwaves are radiated from a circular guide placed on the top side of the vessel ($r = R - R_0 = -4.5$ cm). In order to achieve LHCD, rf waves from a magnetron (0.915 GHz, $P_{LH} \leq 100$ kW, $t \leq 20$ ms) are launched into the plasma with a phased array of four waveguides.

In Figs. 1(a)-1(g) the temporal evolution of plasma parameters with and without P_{EC} is plotted. First, a low-density slide-away discharge (dotted curves) with bulk electron density $\bar{n}_e \sim 2\times10^{12}$ cm^{-3} and temperature $T_e \sim 70$ eV is produced by OH discharge with EC resonance preionization. When P_{EC} is injected after the primary voltage V_1 of the OH transformer is short circuited, the plasma parameters change drastically and a constant plasma current I_p continues to flow with loop voltage $V_L = 0$ as long as P_{EC} is applied (full curves). The data show that the plasma is sustained by EC-driven current only, since no OH current flows for

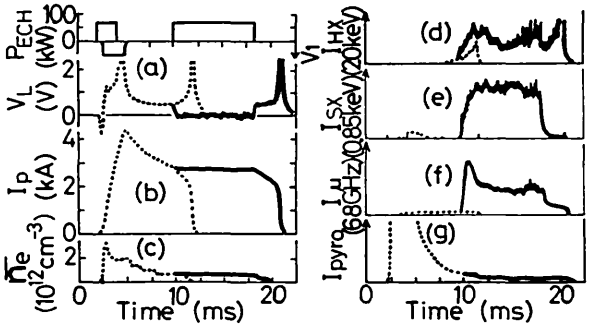

FIG. 1. Temporal evolution of (a) loop voltage V_L, (b) plasma current I_p, (c) line-averaged electron density $\bar{n}_e$ measured by a 4-mm interferometer, (d) hard x-ray emission I_{hx} (20 keV), (e) soft x ray I_{sx} (0.85 keV), (f) electron cyclotron emission I_μ (68 GHz), and (g) pyroelectric signal I_{pyro}. Full curves are for operation with EC-heating power P_{EC} (parallel injection) and dotted ones, without P_{EC}. V_1 is the primary voltage of the OH power supply. $p = 2\times10^{-5}$ Torr in H_2 and additional gas puffing occurs during injection of P_{EC}; $B_T = 12$ kG.

$V_L = 0$. It is noteworthy that in this ECCD plasma strong hard x rays I_{hx} appear and both the soft x ray I_{sx} (0.85 keV) and the EC emission I_μ (68 GHz) increase to more than 10 times those in OH plasma. This result suggests that a suprathermal electron beam carrying the EC-driven current is generated. After P_{EC} is turned off, I_{hx} increases strongly, suggesting that the suprathermal electrons are accelerated by the positive V_L. On the other hand, the pyroelectric signal I_{pyro} and the impurity line I_L(O II–O V) decrease gradually, suggesting that T_e of bulk electrons is nearly the same as that in OH plasma.

In Fig. 2(a) the slope of the x-ray spectrum is about 15 keV and the energy extends to 150 keV in ECCD plasma. Thus, it is concluded that in ECCD plasma the electrons are composed of bulk electrons with $T_e \sim 70$ eV, $\bar{n}_e \sim 0.5\times10^{12}$ cm^{-3}, and suprathermal electrons with $T_e \sim 15$ keV, $n_e \sim 10^{10}$ cm^{-3}, which are carrying $I_p \sim 3$ kA. In addition, the fact that soft x rays up to 100 keV are emitted from the initial OH plasma suggests that weak suprathermal electrons are present and necessary for the formation of ECCD plasma. In fact, for low filling-gas pressure, $p = (2\text{–}5)\times10^{-5}$ Torr, nonthermal emissions I_μ and I_{sx} appear in OH plasma. Then flat-top EC discharge is formed and I_μ and I_{sx} increase strongly when P_{EC} is applied. On the contrary, for $p \geq 6\times10^{-5}$ Torr, both I_μ and I_{sx} are weak. Then I_p decreases with time when P_{EC} is applied.

As P_{EC} increases, the current I_p due to ECCD changes from a decreasing curve to flat-top and then to ramp-up as shown in Figs. 2(b) and 2(c). Correspondingly, the voltage V_L changes from a positive value to a negative value. This behavior is very similar to that in LHCD and shows that I_p is fully sustained by the EC wave. With use of the experimental data of the flat-top discharge, ECCD efficiency is calculated to be

$$\eta = \bar{n}_e I_p R_0 / P_{EC} \sim 1\times10^{-4}\ (10^{20}\ \text{m}^{-2}\ \text{kA/kW}),$$

which is small compared with $\eta \sim 6\times10^{-3}$ for LHCD in the WT-2 tokamak.

The effect of EC heating is examined for various B_T and EC-wave injection methods in Figs. 3(a)–3(c). As B_T increases, the ratio $\Delta I_p/\Delta t$ approaches zero, becomes positive, and then negative. Correspondingly, the voltage V_L varies from positive to negative and then to positive. Also, nonthermal emission I_{sx} becomes intense in the range $\Delta I_p/\Delta t \geq 0$. The flat-top or ramp-up discharge is obtained when B_T is weak and the EC resonance layer is located on the inner side of the torus. Inefficient ECCD under strong B_T may correspond to the theoretical prediction that the EC-heated electrons become trapped on the outer side of the torus.[12] The ECCD efficiency with the EC wave propagating parallel to the electron drift is better than that with the EC wave propagating antiparallel or perpendicular to B_T. Radial profiles of I_{sx} show broad peaks near the plasma center, and Ω_e at the peaks is somewhat smaller than ω. It is concluded that plasma current is generated by EC heating of the suprathermal

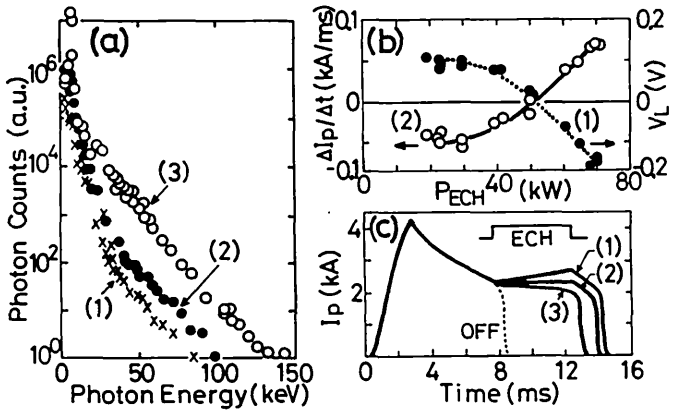

FIG. 2. (a) Energy spectra of x rays emitted from the plasma of Fig. 1 during (1) time $t = 0$–5 ms (startup stage), (2) $t = 5$–10 ms (OH stage), and (3) $t = 10$–15 ms (ECCD stage). (b) (1) Loop voltage V_L and (2) ramp-up rate as a function of P_{EC}. (c) EC-driven current ramp-up, flat-top, and decrease for various P_{EC}: (1) $P_{EC} = 70$ kW, (2) 50 kW, (3) 30 kW.

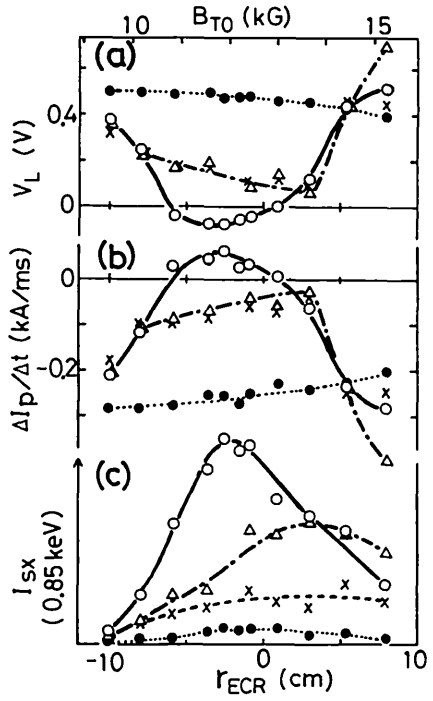

FIG. 3. (a) Loop voltage V_L, (b) time derivative of current $\Delta I_p/\Delta t$, and (c) soft x-ray signal I_{sx} as functions of the field $B_T(r = 0)$ or EC resonance layer r_{ECR}. Open circles are for parallel injection of P_{EC}, triangles for antiparallel injection, and crosses for perpendicular injection. Closed circles are for OH plasma.

electron beam formed in the initial OH plasma. Such a unidirectional electron beam may eliminate the canceling effect of EC-driven current on the opposite side. The fact that the EC-heating effect does not depend strongly on the direction of wave propagation or the polarization (X or O mode) may be ascribed to the reflection of the wave at the vessel wall.

Such an ECCD mechanism is also demonstrated for microwave discharge at EC resonance in the WT-2 tokamak, where a weak current I_p is generated. Here, the toroidal drift of electrons circulating in one direction is canceled by the superposition of a vertical field B_V and an electron beam is formed. The EC-driven current is generated in the direction determined by B_V, independent of the propagation direction of the EC wave.

In contrast with the OH plasma, in the LHCD plasma high-energy electrons in the mildly relativistic range, which carry the current I_p, are produced. Highly efficient ECCD is expected in LHCD plasma, since the EC wave is strongly absorbed by such high-energy electrons and their collisionality decreases further.[13,14] As shown by the dotted curves in Figs. 4(a)–4(f), when P_{LH} is injected into an initial EC-resonance plasma, the current I_p starts up, increases, and a tokamak plasma is formed by rf power alone (so-called rf tokamak[6]). When P_{EC} is applied to the rf tokamak plasma the ramp-up rate of current, $\Delta I_p/\Delta t$, increases, and after termination of the P_{EC} pulse, I_p attains a value higher than that without P_{EC} (solid curves). This increment of I_p is ascribed to the EC-driven current and the voltage V_L, the direction of which is opposed to that of electron drift, increases in proportion to $\Delta I_p/\Delta t$. The electron density $\bar{n}_e$ remains constant. The emissions I_{sx}, I_{hx}, and I_μ increase drastically during EC heating, while, I_{pyro} and I_L(O II–O V) do not change or decrease slightly. These results suggest that high-energy electrons are generated by EC heating, though there is no effect on the bulk electrons.

Measurements show that this EC-driven current is generated when B_T is strong and the EC resonance layer ($\omega = \Omega_e$) is on the outer side of the torus. It is remarkable that radial profiles of I_{sx} and I_{hx} have peaks at higher field positions than the EC reasonance layer. In Fig. 4, the EC resonance layer is located at $r_{ECR} \sim 0.7a$, and peaks of I_{sx} and I_{hx} are at $r \sim 0.3a$ or $\Omega_e/\omega = 1.07$. The change of I_p due to ECCD in the rf tokamak was measured as a function of B_T. When B_T is weak and the EC resonance layer is located on the inner side of the torus ($r_{ECR} \leq 0$), I_p decreases ($\Delta I_p/\Delta t < 0$) during injection of P_{EC}. Here I_{pyro} and I_L(O IV, O V) increase remarkably, while I_μ and I_{sx} do not change, showing that only the bulk electrons are heated at $\Omega_e/\omega \sim 1$.[15] The dependence of the change of I_p due to ECCD on B_T is the same for the various methods of P_{EC} injection. In the rf tokamak, high-

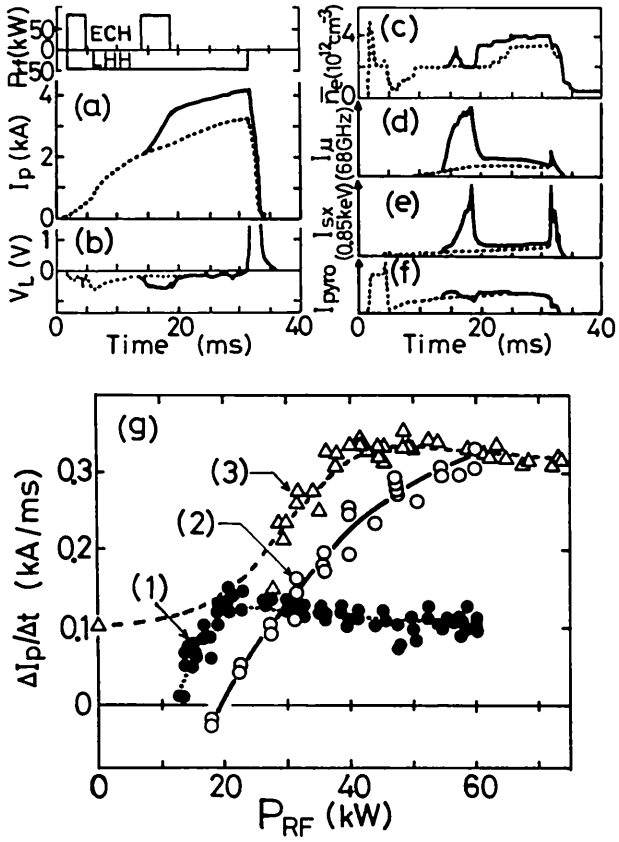

FIG. 4. Temporal evolution of (a) I_p, (b) V_L, (c) $\bar{n}_e$, (d) I_μ (68 GHz), (e) I_{sx} (0.85 keV), and (f) I_{pyro} in the rf tokamak. Solid curves are for operation with P_{EC} (top injection) and dotted ones, without P_{EC}. $p = 6\times10^{-5}$ Torr in H_2 and additional gas puffing is applied during P_{LH}; $B_T = 15$ kG. (g) Ramp-up rate as a function of P_{EC} or P_{LH} in the cases of (1) $P_{EC} = 0$, (2) $P_{EC} = 62$ kW, and (3) $P_{LH} = 60$ kW; $B_T = 15$ kG.

energy electrons are present and strong x rays up to 300 keV are emitted. When P_{EC} is injected in the strong-B_T case, the x-ray emission increases by a factor of 3 in the high-energy range of 20–200 keV, while there is no change below 20 keV.

With consideration of the relativistic effect and Doppler shift, the EC-resonance condition is given by

$$1-(N_{\parallel}v_{\parallel})/c = (\Omega_e/\omega)\{1-(v_{\parallel}^2+v_{\perp}^2)/c^2\}^{1/2}.$$

As the electron energy increases, the resonance occurs at $\Omega_e/\omega > 1$, even if $N_{\parallel}v_{\parallel} > 0$.[13,14] Calculation shows that in the field region of $\Omega_e/\omega = 1.07 \pm 0.05$ in Fig. 4, the energy of resonant electrons is 20–150 keV for $N_{\parallel} = 0.23 \pm 0.1$ and 2–50 keV for $N_{\parallel} = -0.23 \pm 0.1$, where $v_{\perp}^2 = 2v_{\parallel}^2$ is assumed. It is concluded that mildly relativistic electrons generated by lower hybrid waves and drifting along one direction of B_T are heated by EC waves, and then these electrons become more collisionless and carry the EC-driven current efficiently. In Fig. 4(g) the ramp-up rate $\Delta I_p/\Delta t$ is plot-

ted as a function of P_{rf} (P_{LH} or P_{EC}). For an rf tokamak discharge ($P_{EC}=0$), as P_{LH} increases $\Delta I_p/\Delta t$ increases at first, and then attains a constant value (curve 1). When a constant P_{EC} is superposed, $\Delta I_p/\Delta t$ increases with P_{LH} (curve 2) and exceeds that with $P_{EC}=0$. When the rf tokamak is sustained by constant P_{LH}, the current ramp-up rate increases with P_{EC} and attains a constant value (curve 3). If it is assumed that the change of ramp-up rate with respect to P_{rf}, $d(\Delta I_p/\Delta t)/dP_{rf}$, is proportional to the efficiency of rf CD, η_{rf}, then both η_{EC} with a constant P_{LH} and η_{LH} with a constant P_{EC} are nearly equal to η_{LH} without P_{EC} in the unsaturated region. It is suggested theoretically[10] that

$$\eta_{EC}/\eta_{LH} \sim \tfrac{3}{4}\{1+(v_\perp/2v_\parallel)^2\}^{-1} \sim 1,$$

which is consistent with the experimental results.

In conclusion, EC-driven current is generated in two types of plasma. First, such current is generated by EC heating of the suprathermal electron beam, and the current I_p is sustained or ramped up when P_{EC} is injected into the plasma after OH power is shut off. Second, EC-driven current is generated by EC heating of the mildly relativistic electron beam, and the ramp-up rate of I_p increases when P_{EC} is injected into the rf tokamak. Such an enhancement of LHCD efficiency combined with EC heating is quite important for a new, useful, and efficient method of rf CD, especially on large tokamaks with high T_e and enough electrons in the mildly relativistic range. Further, this result may support the idea that the efficiency of beam-injection or alpha-particle current drive increases when ion-cyclotron heating is superposed in order to compensate for the energy loss of ions.[16]

This work is supported by a Grant-in Aid for Scientific Researches from the Ministry of Education of Japan.

---

[a]Permanent address: Osaka Institute of Technology, Osaka 535, Japan.

[b]Permanent address: Plasma Research Center, The University of Tsukuba, Ibaraki 305, Japan.

[1]*Non-Inductive Current Drive in Tokamaks,* edited by D. F. H. Start (Culham Laboratory, Abingdon, United Kingdom, 1983), Vols. 1 and 2.

[2]M. Nakamura *et al.*, Phys. Rev. Lett. **47**, 1902 (1981), and J. Phys. Soc. Jpn. **51**, 3696 (1982), and **53**, 3399 (1984).

[3]S. Bernabei *et al.*, Phys. Rev. Lett. **49**, 1255 (1982).

[4]M. Porkolab *et al.*, Phys. Rev. Lett. **53**, 450 (1984).

[5]M. J. Mayberry *et al.*, Phys. Rev. Lett. **55**, 829 (1985).

[6]S. Kubo *et al.*, Phys. Rev. Lett. **50**, 1994 (1983), and J. Phys. Soc. Jpn. **53**, 1047 (1984).

[7]K. Toi *et al.*, Phys. Rev. Lett. **52**, 2144 (1984).

[8]N. J. Fisch and C. F. F. Karney, Phys. Rev. Lett. **54**, 897 (1985).

[9]F. C. Jobes *et al.*, Phys. Rev. Lett. **55**, 1295 (1985).

[10]N. J. Fisch and A. H. Boozer, Phys. Rev. Lett. **45**, 720 (1980).

[11]C. F. F. Karney and N. J. Fisch, Nucl. Fusion **21**, 1549 (1981).

[12]M. W. Alcock *et al.*, in *Proceedings of the Ninth International Conference on Plasma Physics and Controlled Nuclear Fusion Research, Baltimore, 1982* (International Atomic Energy Agency, Vienna, 1983), Vol. 2, p. 51.

[13]I. Fidone *et al.*, Phys. Fluids **26**, 3284 (1983), and **27**, 661, 2468 (1984), and Nucl. Fusion **25**, 127 (1985).

[14]R. A. Cairns *et al.*, Phys. Fluids **26**, 3475 (1983).

[15]A. Ando *et al.*, Nucl. Fusion **26**, 107 (1986).

[16]K. Okano *et al.*, Nucl. Fusion **23**, 235 (1983).